 CMC, vol.39, no.1, pp.3-20, 2014

Dynamic Instability of Rectangular Composite Plates under Parametric Excitation

Meng-Kao Yeh[1], Chia-Shien Liu[2] and Chien-Chang Chen[3]

Abstract: The dynamic instability of rectangular graphite/epoxy composite plates under parametric excitation was investigated analytically and experimentally. In analysis, the dynamic system of the composite plate, obtained based on the assumed-modes method, is a general form of Mathieu's equation, including parametrically excited terms. The instability regions of the system, each separated by two transition curves, were found to be functions of the modal parameters of the composite plate and the position and the excited amplitude of the electromagnetic device on the composite plates. The fiber orientation, the aspect ratio and the layer numbers of the composite plates were varied to assess their effects on the dynamic instability behavior of the composite plates. In experiment, an electromagnetic device, acting like a spring with alternating stiffness, was used to parametrically excite the composite plates. The frequency and the amplitude of the excitation force were accurately controlled by the AC current flowing through the coil of the electromagnetic device. Since the excitation force was a transversely non-contact electromagnetic force, the disturbances induced by the eccentricity of the usual planar excitation force and by the geometric imperfection of the composite plate were effectively avoided. The experimental results, for the cases of twice the fundamental frequency, were found to agree well with the analytical ones. The excitation frequencies at tip of instability regions decrease as the fiber orientation increases for composite plates with $[\pm\theta_2]_s$ lamination at bending mode; while the excitation frequencies increase to a maximum at 45^o fiber orientation for composite plates with $[\pm\theta_2]_s$lamination at torsional mode. The excitation frequency at tip of instability regions decreases for higher aspect ratios and thinner composite plates.

Keywords: Dynamic Instability, Composite Plate, Parametric Excitation, Elec-

[1] Department of Power Mechanical Engineering, National Tsing Hua University, Hsinchu 30013 Taiwan.

[2] Department of Power Mechanical Engineering, National Tsing Hua University, Hsinchu 30013 Taiwan.

[3] Department of Mechanical Engineering, Dahan Institute of Technology, Hualien 971 Taiwan.

tromagnetic Spring.

1 Introduction

The problem of dynamic instability has been playing an important role for the safety of structures. Bazant (2000) reported the following structural failure examples due to their instability hehavior: the resonance of Tacoma Narrows Bridge due to air flow which resulted in its failure in 1940; the failure of space frame, Hartford Arena, in 1978; the failure of Quebec bridge at St. Lawrence in 1907. Bolotin (1965) summarized the parametrically excited instability problems for various structural elements. Evan-Iwanowski (1965) and Nayfeh and Mook (1979) also reviewed the similar problems. The governing equation of the parametrically excited instability problem is a Mathieu equation, which was analyzed by many researchers [Hsu (1963); Nayfeh and Mook (1977); Fox (1990)] to obtain the system instability solution for the problem of multiple degrees of freedom.

Researchers also investigated the parametrically excited instability problem of the basic structural elements, such as beams, columns, plates and shells for different material properties, different boundary conditions, and different excitation forces analytically. Yeh and Chen (1998) and Chen and Yeh (1999) investigated analytically a general column under a periodic load in the direction of the tangency coefficient at any axial position; they also assessed the simple and combination resonances of a general column carrying an axially oscillating mass and gave physical explanations of the parametric resonances by viewing the system energy. Ganapathi and Balamurugan (1998) investigated the dynamic instability of circular cylindrical shells using the finite element method. Deolasi and Datta (1995; 1997) studied the simple and combination resonances for a simply-supported rectangular plate under nonuniform edge loading with damping and under localized edge loading.

As the rapid development of aeronautical technology, although the basic structural elements (beams, columns, plates and shells), made from traditional metal materials, have enough strengths in design, their relative heavy weights make themselves not suitable in aeronautical use. Composite materials, with high specific strength, high specific stiffness and the ability of variable lamination to have required mechanical property, becomes an competitive substitute for use in various aerospace substructures. The composite structure has excellent mechanical property from static analysis. However, the composite structure may become unstable due to external dynamic disturbances resulted from external resonance or parametrically excited resonance, caused by periodic forces. Srinivasan and Chellapandi (1986) investigated the dynamic instability of composite plate by the finite strip method. Chen and Yang (1990) studied the dynamic stability of angle-ply composite plates under compressive forces by finite element method. Moorthy and Reddy (1990)

investigated the parametric instability of composite plates with transverse shear deformation. As the instability experiment is conserned, Bassiouni *et al* (1999) studied the dynamic instability of composite beams analytically and experimentally. Chen and Yeh (2001) investigated the parametrically excited instability problem of beams under electromagnetic excitation analytically and experimentally. Yeh and Kuo (2004) studied the instability problem of composite beams analytically and experimentally.

From the above-mentioned literature, most researchers investigated the parametrically excited instability problem of structures analytically or numerically. The experimental work on the dynamic instability for parametrically excited composite plate is rather limited. In this paper, the dynamic instability of rectangular graphite/epoxy composite plates under parametric excitation was investigated analytically and experimentally. The electromagnetic device, acting as a spring of variable stiffness, was used as a non-contacting transversely parametric exciter in experiment, and the effects caused by the geometric imperfection, the eccentricity of the planar excitation forces could be avoided.

2 Instability Analysis of Composite Plate

The dynamic instability equation of rectangular composite plate is obtained based on the assumed-modes method. The finite element code ANSYS® was used to obtain the natural frequencies and natural modes of the composite plate and finally the instability regions of the composite plate under parametric excitation were found.

The composite plate under electromagnetic excitation is idealized as shown in Figure 1, with left end fixed and free at right end. The electromagnetic device was modeled as a concentrated mass$m_o$and a spring with stiffness $k(t)$ connected at point P at the mid-plane of composite plate. The composite plate has length a, width b, thickness h, mass M The composite plate is made from the prepreg, which is assumed transversely isotropic with material principal axis on the $x-y$ plane. The composite plate, symmetric to the mid-plane, satisfies the Kirchhoff assumption. The gravitational effect was ignored in analysis.

The dynamic equation of the composite plat, without spring $k(t)$, can be expressed as

$$\begin{aligned} &D_{11}\frac{\partial^4 w}{\partial x^4}+2\left(D_{12}+2D_{66}\right)\frac{\partial^4 w}{\partial x^2\partial y^2}+D_{22}\frac{\partial^4 w}{\partial y^4} \\ &+\left[\rho+m_0\delta\left(x-x_0\right)\delta\left(y-y_0\right)\right]\frac{\partial^2 w}{\partial t^2}+c\frac{\partial w}{\partial t}=0 \end{aligned} \tag{1}$$

in which D_{11} D_{12} D_{22} and D_{66} obtained from the integration of transformed lamina stiffnesses in the thickness direction, represent the laminate-bending stiffnesses of

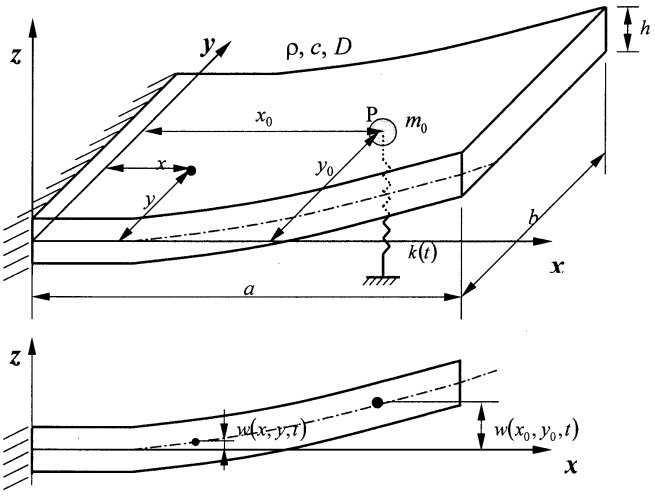

Figure 1: Idealized model for composite plate under an electromagnetic excitation

the composite plate; ρ and c are the density and damping coefficient of the composite plate; $\delta(x-x_o)$ and $\delta(y-y_o)$ are unit pulse functions; (x_o, y_o) represents the central position of the electromagnetic device with mass m_o at point P

2.1 Finite Element Modal Analysis

Using the assumed mode method [Craig (1981)], the transverse displacement of the composite plate $w(x,y,t)$ can be expressed as the summation of the normalized modal vector $\phi_n(x,y)$ multiplied by its corresponding displacement component $V_n(t)$ as

$$w(x,y,t) = \sum_{n=1}^{\infty} \phi_n(x,y) V_n(t) \tag{2}$$

where $V_n(t)$ is function of time only. For the specified boundary condition, fixed at left and free at right, the orthogonal function ϕ_n(x, y) must satisfy

$$\int_0^b \int_0^a [\rho + m_0 \delta(x-x_0)\ \delta(y-y_0)]\, \phi_n(x,y)\, \phi_m(x,y)\, dxdy = \delta_{nm} \tag{3}$$

Since one end of the composite plate is clamped and the other three sides free, the exact solution for the modal shapes of transverse vibration is not available and the finite element analysis was used to obtain the vibration modes ϕ_n(x, y) of the composite plate. The three-dimensional Shell99 element was used in the analysis.

Each element has 8 nodes and each node has 6 degrees of freedom. The attached electromagnetic device was modeled as a concentrated mass, element type Mass21, located at the center of the device. After applying the boundary conditions, the natural frequencies and the corresponding modal vectors of the composite plate can be obtained using ANSYS®code. Besides, the modal vector satisfies the normalized orthogonal condition.

2.2 Parametrically Excited Dynamic Equation

Since the system considered contains an electromagnetic spring and no external forces, the system dynamic equation can be obtained below, similar to the case for the composite beam [Yeh and Kuo (2004)]

$$\ddot{V}_n(t) + d_n\dot{V}_n(t) + \omega_n^2 V_n(t) + k(t)\sum_m \phi_m(x_0,y_0)\,\phi_n(x_0,y_0)\,V_m(t) = 0 \text{ for } n = 1,2,\ldots \tag{4}$$

in which $d_n = c/\rho$ is the modal damping coefficient; ω_n is the undamped natural frequency of the laminated plate system. The variables are nondimensionalized in the following form.

$$\xi = \frac{x}{a};\quad \eta = \frac{y}{b};\quad \tau = \omega_1 t;\quad \mu_n = \frac{d_n}{2\omega_1};\quad \bar{\omega}_n = \frac{\omega_n}{\omega_1};\quad \varepsilon(\tau) = \frac{k(t)}{2M\omega_1^2};$$
$$f_{nm} = M\phi_m(x_0,y_0)\,\phi_n(x_0,y_0) = M\phi_m(\xi_0,\eta_0)\,\phi_n(\xi_0,\eta_0)$$

where ω_1 is the fundamental frequency. Then the system dynamic equation becomes

$$\ddot{V}_n(\tau) + 2\mu_n\dot{V}_n(\tau) + \bar{\omega}_n^2 V_n(\tau) + 2\varepsilon(\tau)\sum_m f_{nm}V_m(\tau) = 0 \text{ for } n = 1,2,\ldots \tag{5}$$

If the stiffness of spring is a constant, $\varepsilon(\tau) = \varepsilon$. The natural frequencies of the transverse vibration of composite plate shift slightly due to the spring effect. This could be used to identify the spring stiffness ε in experiment. If the spring has variable stiffness, $\varepsilon(\tau) = \varepsilon\cos\bar{\omega}\tau$, then equation (5) becomes

$$\ddot{V}_n(\tau) + 2\mu_n\dot{V}_n(\tau) + \bar{\omega}_n^2 V_n(\tau) + 2\varepsilon\cos\bar{\omega}\tau\sum_m f_{nm}V_m(\tau) = 0 \text{ for } n = 1,2,\ldots \tag{6}$$

The above equation is a Mathieu equation, in which the excitation term contains the modal displacement V_n and the parametric excitation coefficient f_{nm}

2.3 Criterion for Parametric Instability

After obtaining the parametric excitation coefficient f_{nm}, the instability bandwidth parameter G_{nm} can be calculated. The instability regions can be found from the instability bandwidth parameter G_{nm}, the amplitude of the spring, and the natural frequencies of the composite plate $\bar{\omega}_n$, $\bar{\omega}_m$ [Chen and Yeh (2001); Yeh and Kuo (2004)]

(a) For Simple Resonance

When the excitation frequency $\bar{\omega}$ is close to twice the natural frequency $2\bar{\omega}_n$ and the instability bandwidth parameterG_{nn} is defined as

$$G_{nn} = \begin{cases} \left(\frac{f_{nn}}{\bar{\omega}_n}\right)^2 - 4\left(\frac{\mu_n}{\varepsilon}\right)^2, \ \mu_n \neq 0 \\ \left(\frac{f_{nn}}{\bar{\omega}_n}\right)^2, \ \mu_n = 0 \end{cases} \tag{7}$$

The transition curves separate the stable and unstable regions are

$$\bar{\omega} = 2\bar{\omega}_n \pm \varepsilon G_{nn}^{1/2}, \quad \text{when } G_{nn} > 0 \tag{8}$$

(b) For Combination Resonance of Summed Type

When the excitation frequency $\bar{\omega}$ is close to the sum of two natural frequencies $\bar{\omega}_n + \bar{\omega}_m$ and the instability bandwidth parameter G_{nm} is defined as

$$G_{nm} = \begin{cases} \dfrac{(\mu_n + \mu_m)^2}{\mu_n \mu_m} \left[\dfrac{f_{nm} f_{mn}}{4\bar{\omega}_n \bar{\omega}_m} - \dfrac{\mu_n \mu_m}{\varepsilon^2}\right], & \mu_{\mathrm{n}} \text{ and } \mu_m \neq 0 \\ \dfrac{f_{nm} f_{mn}}{4\bar{\omega}_n \bar{\omega}_m}, & \mu_n \text{ or } \mu_{\mathrm{m}} = 0 \end{cases} \tag{9}$$

The transition curves separate the stable and unstable regions are

$$\bar{\omega} = \bar{\omega}_n + \bar{\omega}_m \pm \varepsilon G_{nm}^{1/2}, \quad \text{when } G_{nm} > 0 \tag{10}$$

(c) For Combination Resonance of Difference Type

When the excitation frequency $\bar{\omega}$ is close to the difference of two natural frequencies $\bar{\omega}_n - \bar{\omega}_m$, $(\bar{\omega}_n > \bar{\omega}_m)$ and the instability bandwidth parameter G_{nm} is defined as

$$G_{nm} = \begin{cases} \dfrac{(\mu_n + \mu_m)^2}{\mu_n \mu_m} \left[-\dfrac{f_{nm} f_{mn}}{4\bar{\omega}_n \bar{\omega}_m} - \dfrac{\mu_n \mu_m}{\varepsilon^2}\right], & \mu_{\mathrm{n}} \text{ and } \mu_m \neq 0 \\ -\dfrac{f_{nm} f_{mn}}{4\bar{\omega}_n \bar{\omega}_m}, & \mu_n \text{ or } \mu_{\mathrm{m}} = 0 \end{cases} \tag{11}$$

The transition curves separate the stable and unstable regions are

$$\bar{\omega} = \bar{\omega}_n - \bar{\omega}_m \pm \varepsilon G_{nm}^{1/2}, \quad \text{when } G_{nm} > 0 \tag{12}$$

The instability regions of the system, each separated by two transition curves, were found to be functions of the modal parameters of the composite plate and the position and the excitation amplitude of the electromagnetic device on the composite plates.

3 Experiment

In addition to the analysis, parametrically-excited instability experiments were performed to verify the analytical results. The instability experiment for composite plate follows the basic procedure reported in [Chen and Yeh (2001); Yeh and Kuo (2004)] except the composite plate specimens were used in this study. The equipment includes a hot press to make the composite plate specimen, an air compressor to provide uniform pressure and a vacuum pump to extract the air generated during the molding of plate specimen.

3.1 Composite Plate Specimen

The thermosetting graphite/epoxy prepreg, 0.12 mm thick approximately, was used in making the composite plate. The prepreg was cut into the required size and stacked to form the composite plate in the hot press. Finally, the composite plate was cut and trimmed to the desired specimen size for experiment.

The material properties of the composite plate were measured on a tensile testing machine according ASTM D3039-76 (1983) and ASTM D3518-76 (1983). Each layer of the composite plate is assumed to be transversely isotropic [Gibson (2007)]. Five material constants, E_{11}, E_{22}, G_{12}, ν_{12}, and ν_{23} are needed. ν_{23}, which is difficult to measure in experiment, is assumed to be equal to ν_{12} as previously reported [Yeh and Tan (1994)]. Each material constant was measured five times and average value was obtained. The longitudinal modulus is E_{11}=147.56$\pm$0.45 GPa, the Poisson's ratio ν_{12}=0.283$\pm$0.0013, the transverse modulus E_{22}=9.31$\pm$0.06 GPa, and the shear modulus G_{12}=5.70$\pm$0.04 GPa.

3.2 Dynamic Instability Experiment

The equipment used in the dynamic instability experiment of the composite plate includes a dynamic signal analyzer, an AC/DC power supply, an accelerator, an impact hammer and force sensor, a signal conditioner, and an electromagnetic device acting as a spring. The electromagnetic spring is made from a pair of magnets and a pair of coils. The magnets are fixed on the supporting frame; while the coils are

wound on a plastic square frame glued on the composite plate specimen. When a DC current flows through the coils, the coils become an electromagnet. The force between the electromagnet and the magnet fixed on the support makes the device to act like a spring [Chen and Yeh (2001)]. When an AC current flows through the coils, the coils become an electromagnetic spring of variable stiffness, which was used as a non-contacting parametric exciter in experiment. Since the excitation force acted on the composite plate transversely, the effects caused by the geometric imperfection, the eccentricity of the planar excitation force could be avoided in experiment.

Before the instability experiment, the characteristics of the electromagnetic spring were identified using a DC power supply and an impact hammer. A DC current was applied through the coils to form an electromagnetic spring and the natural frequencies of the plate specimen were found using an impact hammer. The transverse fundamental frequency of the composite plate was calculated using ANSYS® A relation between the transverse fundamental frequency and the DC current was established first. Secondly, the relation between the transverse fundamental frequency and the stiffness of the electromagnetic spring was obtained. Finally, the relation between the stiffness of the electromagnetic spring ε and the current Ithrough the coils was identified below

$$\varepsilon = 0.02281\,I - 0.00094 \tag{13}$$

Figure 2 shows the relation between the stiffness of the electromagnetic spring and the DC current through the coils for composite plate ($[0^\circ]_8$, 20×20.2 cm)

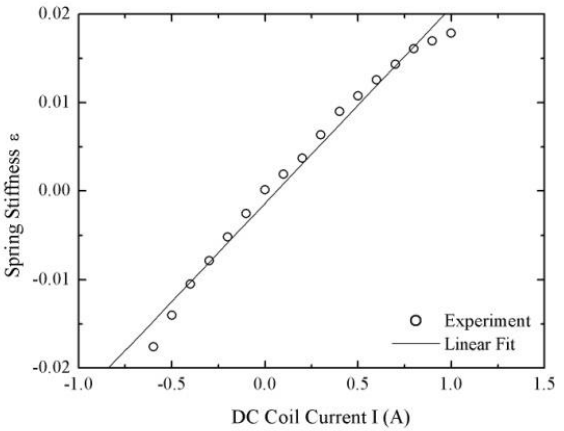

Figure 2: Electromagnetic spring stiffness versus DC coil current for composite plate ($[0^\circ]_8$, 20×20.2 cm)

Figure 3 shows experimental setup for composite plate under electromagnetic excitation. Figure 4 shows the schematic for measuring dynamic instability of composite plate under electromagnetic excitation. An AC power supply was used to make the electromagnetic device a sinusoidal exciter on the composite plate. The frequency of AC current was applied and increased slightly step-by-step from the lower limit to the higher limit in the specified frequency range. At each excitation frequency, the amplitude of the AC current was increased from zero to a saturated value to observe the dynamic response of the composite plate. The position of excitation, where the electromagnetic device located, was chosen away from the fixed end to obtain the vibration signals more easily. The instability of the composite plate was observed when its vibrating amplitude increased abruptly. Once the instability occurred, the current was cut off immediately. The excitation frequency and the current amplitude were recorded. This procedure was repeated to obtain the instability region for each composite plate. The fiber orientation, the aspect ratio and the layer numbers of composite plate, were varied to study their effects on the instability behavior of the composite plates.

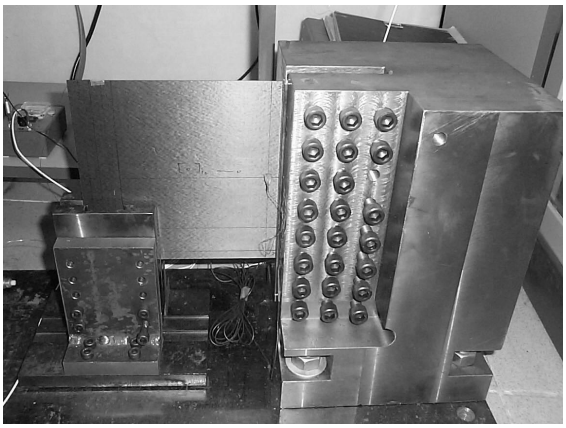

Figure 3: Experimental setup for composite plate under electromagnetic excitation.

4 Results and Discussion

The natural frequencies and the modal shapes of composite plate were found first using the finite element code ANSYS®; from this the instability regions of the composite plate were obtained as described in the previous analysis section. The parameters, including the fiber orientation, the aspect ratio and the layer numbers of composite plate, are considered in this study.

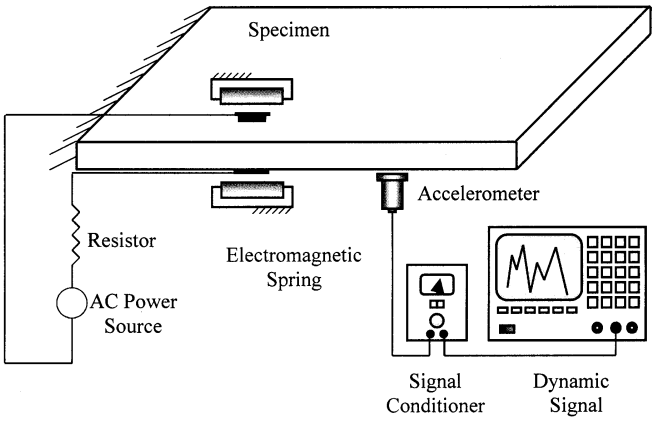

Figure 4: Schematic for measuring dynamic instability of composite plate under electromagnetic excitation.

4.1 Finite Element Analysis

In ANSYS, Shell99 elements were used for the composite plate. Mass21 element was used for the electromagnetic device. For Shell99, nine constants (E_{11}, E_{22}, E_{33}, ν_{12}, ν_{23}, ν_{13}, G_{12}, G_{23}, G_{13}) are needed to input, in which E_{11}, E_{22}, ν_{12} and G_{12} were obtained from experiment. Other constants were found according to the specially orthotropic assumption as follows.

$$E_{33} = E_{22},\ \nu_{23} = \nu_{12},\ \nu_{13} = \frac{\nu_{12} E_{22}}{E_{33}},\ G_{23} = \frac{E_{22}}{2(1+\nu_{23})},\ G_{13} = G_{12} \tag{14}$$

There were total of 196 elements for a composite plate with electromagnetic device in modal analysis. Figure 5 shows the fundamental and the second vibration modes of composite plate ($[0^\circ]_8$, a=20 cm, b=20.2 cm). The fundamental mode is a bending type and the second mode a torsional one. The natural frequencies of composite plate with the mass of electromagnetic device are lower than those without mass. The frequencies become higher or lower as the fiber orientation increases, depending on the mode shape. The natural frequencies increase as the layer number of composite plate increases, since the thicker composite plates have higher stiffness.

4.2 Parametric Instability Regions of Composite Plate

The parametric instability regions of composite plates were obtained from their modal parameters at the position of electromagnetic device, from which the parametric excitation coefficient f_{nm}, the instability bandwidth parameter G_{nn} and the

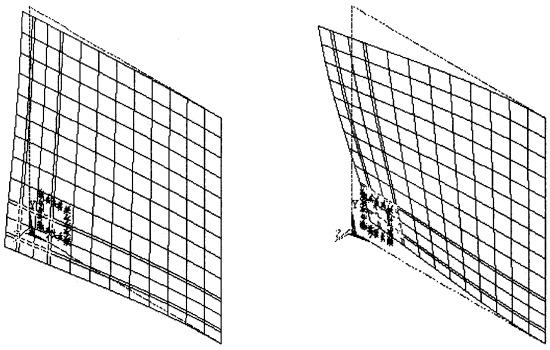

(a) fundamental mode (b) second mode

Figure 5: Vibration modes of composite plate ($[0^{\circ}]_8$, a=20 cm, b=20.2 cm)

transition curves separate the stable and unstable regions were found. In this study, the simple resonances, $2\omega_1$, $2\omega_2$, $2\omega_3$, and the combination resonances at $\omega_1+\omega_2$, $\omega_1+\omega_3$, and $\omega_2+\omega_3$ are discussed.

Various composite plate specimens were analyzed for their instability behavior. For example, Figure 6 shows the dynamic instability regions at simple and combination resonant frequencies of the composite plate with $[\pm(30^o)_2]_s$, length a=20 cm, width b=20 cm. $\bar{\omega}$ is the ratio between the parametric excitation frequency and the fundamental natural frequency ω_1. $\bar{\omega}_2$ and $\bar{\omega}_3$ denote the second and the third resonance frequencies after nondimensionalization by ω_1. From equations (6) and (5), the amplitude ε in Figure 6 represents the spring stiffness. Since the instability bandwidth parameter G_{nm} was found negative, no combination resonance of difference type was obtained in this problem. Figure 7 shows the instability region at $2\bar{\omega}_1$ in Figure 6 for the composite plate with $[\pm(30^o)_2]_s$. The amplitude ε was calculated from equation (10) for different current value; then the instability region was obtained from equation (5). A maximum instability region occurs at twice the fundamental frequency $2\bar{\omega}_1$. The reason is that the instability bandwidth parameter G_{nm}, related with the mass of the plate and the modal parameters at the position of the electromagnetic device only, has higher value for the fundamental bending mode. The little shift between the analytical and experimental results was probably due to the assumed perfectly fixed boundary condition used in the analysis. In general, the experimental results agree well with the analytical ones for the simple resonances at twice the fundamental frequency.

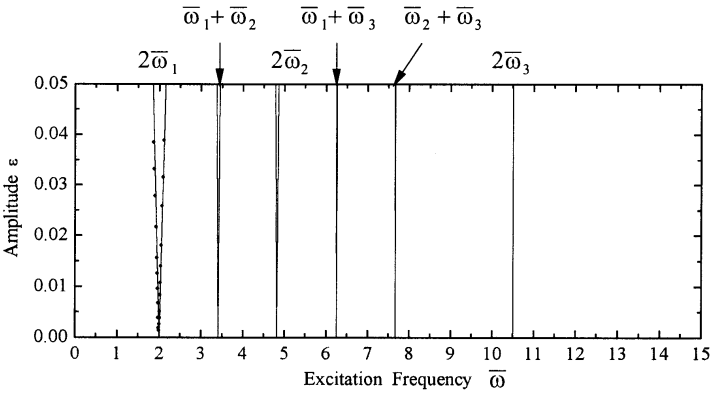

Figure 6: Dynamic instability regions of composite plate with$[\pm(30^o)_2]_s$. _____ analytical results; ..... experimental results.

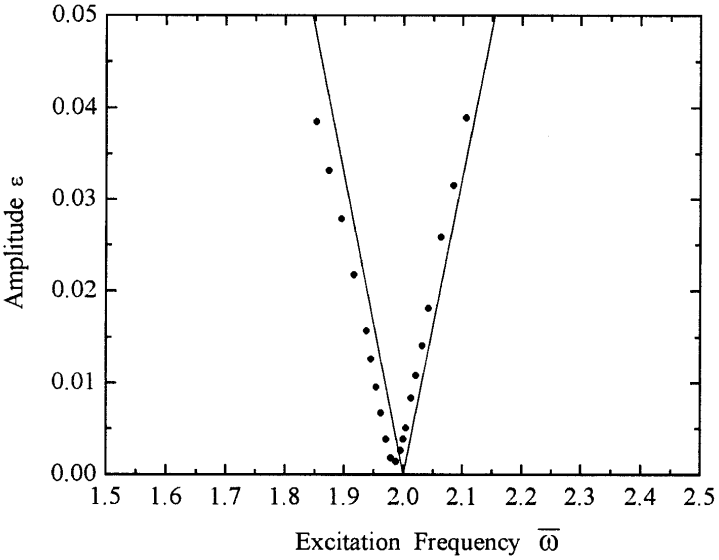

Figure 7: instability region at $2\bar{\omega}_1$ for the composite plate with $[\pm(30^o)_2]_s$._____ analytical results; ..... experimental results.

4.2.1 Effect of Fiber Orientation

Five fiber angles (θ=0˚, 30˚, 45˚, 60˚, 90˚), were varied to assess their effects on the instability behavior of composite plates ($[\pm\theta_2]_s$, a=20 cm, b=20.1 cm). The fundamental frequencies, from $[0^\circ]_8$ to $[90^\circ]_8$ are 33.84 Hz, 24.37 Hz, 17.74 Hz, 11.71 Hz, 8.60 Hz, respectively. The analytical and experimental excitation frequencies for different fiber orientation of composite plates are shown in Table 1. Figure 8 shows the excitation frequency at the tip of each instability region versus fiber orientation of composite plates. The excitation frequencies include the simple and the combination resonances. The experimental results agree well with the analytical ones at twice the fundamental frequency.

Table 1: Analytical and experimental excitation frequency for different fiber orientation of composite plates

Fiber orientation	$2\omega_1$	$\omega_1+\omega_2$	$2\omega_2$	$\omega_1+\omega_3$	$\omega_2+\omega_3$	$2\omega_3$	$2\omega_{1,exp}$
0°	67.7	78.8	89.9	122.2	133.3	176.7	59.8
30°	48.7	83.1	117.4	152.4	186.8	256.1	47.2
45°	35.5	79.9	124.4	130.2	174.7	225.0	33.0
60°	23.4	64.2	105.0	88.4	129.2	153.4	23.9
90^o	17.2	34.1	50.9	66.5	83.3	115.7	18.3

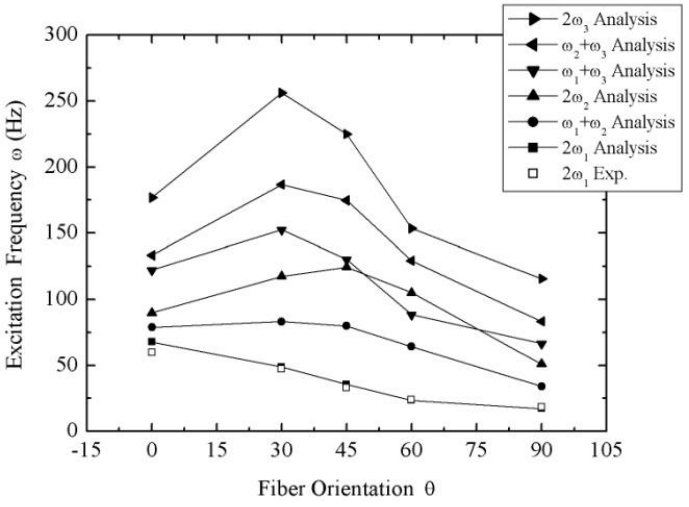

Figure 8: Excitation frequency versus fiber orientation of composite plates.

The excitation frequency varies with the fiber orientation of the composite plate, depending on the mode shape. The excitation frequency decreases with the fiber orientation of the composite plate at twice the fundamental frequency $2\omega_1$ as expected since this bending mode has the highest rigidity at θ=0°. The excitation frequency reaches a maximum at θ=45° for the simple resonance $2\omega_2$ due to the torsional nature of the second mode. The excitation frequency reaches a maximum at θ=30° for the third simple resonance $2\omega_3$ due to the complex nature of the third mode shape.

4.2.2 *Effect of Aspect Ratio*

The aspect ratio was varied to evaluate their effects on the instability behavior of composite plates ($[0^\circ]_8$, a=20 cm, b=20.2 cm). The aspect ratios (a/b) used were 1.0, 0.9, 0.8, 0.7, 0.6 and 0.5, in which the experiment was unable to perform due to limited space on the fixture for a/b= 0.6 and 0.5. The analytical and experimental excitation frequencies for different aspect ratio of composite plates are shown in Table 2. Figure 9 shows the excitation frequency at the tip of each instability region versus aspect ratio of composite plates. The excitation frequencies of both the simple and the combination resonances decrease for larger aspect ratios, i.e., for the longer plates, which possess lower natural frequencies at a fixed width.

Table 2: Analytical and experimental excitation frequency for different aspect ratio of composite plates.

Aspect ratio	$2\omega_1$	$\omega_1+\omega_2$	$2\omega_2$	$\omega_1+\omega_3$	$\omega_2+\omega_3$	$2\omega_3$	$2\omega_{1,exp}$
0.5	236.9	277.4	317.9	312.3	352.8	387.7	–
0.6	170.0	197.2	224.3	234.9	262.1	299.9	–
0.7	128.9	148.5	168.1	188.4	208.0	247.8	121.8
0.8	101.4	116.7	131.9	158.0	173.3	214.6	94.7
0.9	82.0	94.7	107.3	137.2	149.8	192.3	70.3
1.0	67.7	78.8	89.9	122.2	133.3	176.7	59.8

4.2.3 *Effect of Number of Layers*

The number of layers of the composite plate was varied as 4, 8, 12 and 16 to investigate their effects on the instability behavior of composite plates ($[0^\circ]_8$, a=20 cm, b=20 cm). It was observed that a maximum instability region occurred at twice the fundamental frequency $2\bar{\omega}_1$. The analytical and experimental excitation frequencies for different number of layers of composite plates are shown in Table 3.

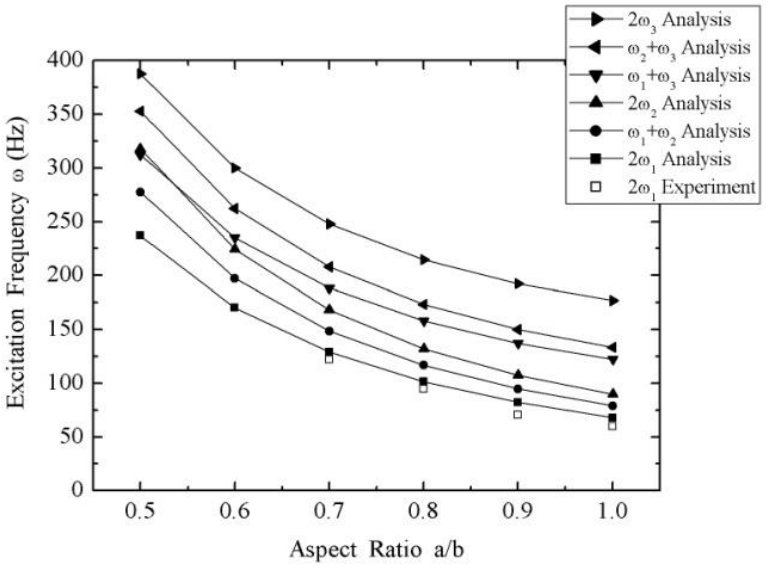

Figure 9: Excitation frequency versus aspect ratio of composite plates.

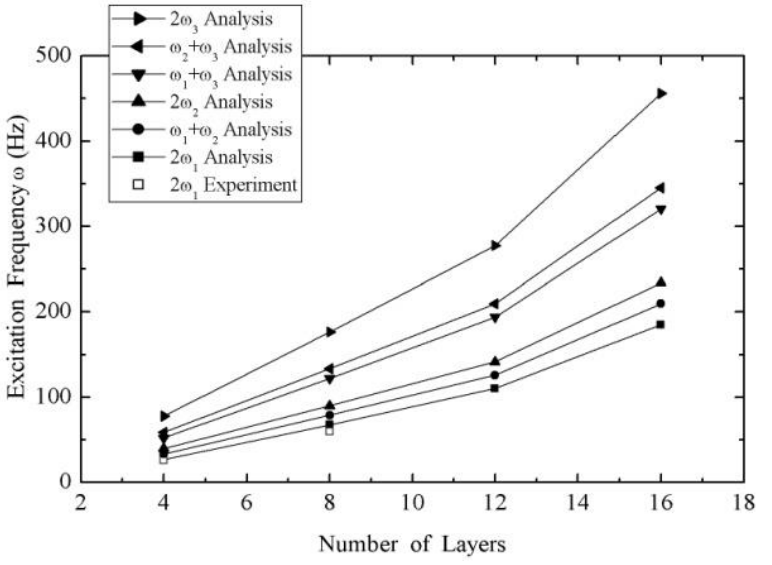

Figure 10: Excitation frequency versus number of layers of composite plates.

Figure 10 shows the excitation frequency at the tip of each instability region versus number of layers of composite plates. The excitation frequencies of both the simple and the combination resonances increase for thicker composite plates. The thicker plates have larger rigidity, and thus higher natural frequencies for the simple and the combination resonances.

Table 3: Analytical and experimental excitation frequency for different number of layers of composite plates.

Layers	$2\omega_1$	$\omega_1+\omega_2$	$2\omega_2$	$\omega_1+\omega_3$	$\omega_2+\omega_3$	$2\omega_3$	$2\omega_{1,exp}$
4	26.7	33.3	39.9	52.2	58.8	77.7	25.8
8	67.7	78.8	89.9	122.2	133.3	176.7	59.8
12	110.1	125.8	141.6	193.9	209.6	277.6	-
16	185.0	209.5	234.0	320.5	345.0	456.0	-

5 Conclusions

In this paper, the dynamic instability of rectangular graphite/epoxy composite plates under parametric excitation was investigated analytically and experimentally. The parameters, including the fiber orientation, the aspect ratio and the layer numbers, were considered to evaluate their effects on the dynamic instability behavior of the composite plates. The following conclusions can be drawn.

1. The instability regions agreed well with the analytical ones for the simple resonances at twice the fundamental frequency. The non-contacting electromagnetic exciter used in experiment acted on the composite plate transversely, the effects caused by the geometric imperfection, the eccentricity of the planar excitation forces could be avoided effectively.

2. The effect of the fiber orientation on the instability region depends on the mode shapes of the composite plates. The excitation frequency decreases with the fiber orientation of the composite plate with $[\pm\theta_2]_s$ for the bending mode instability and reaches a maximum at θ=45° for the torsional mode instability.

3. The excitation frequency at the tip of each instability region decreases for higher aspect ratios.

4. The excitation frequency at the tip of each instability region increases for thicker composite plates.

Acknowledgement: The authors would like to thank the National Science Council, Taiwan, the Republic of China through grant NSC 99-2221-E-007-042-MY3, for supporting this work.

References

ANSYS Theory Reference. 001369. Twelfth. SAS IP, Inc.

ASTM D3039-76 (1983): Standard Test Method for Tensile Properties of Fiber-Resin Composites. *Annual Book of ASTM Standards*, Section 3, vol. 15.03, pp.162-165.

ASTM D3518-76 (1983): Standard Practice for Inplane Shear Stress-strain Response of Unidirectional Reinforced Plastics. *Annual Book of ASTM Standards*, Section 3, vol. 15.03, pp. 202-207.

Bassiouni, A. S.; Gad-Elrab, R. M.; Elmahdy, T. H. (1999): Dynamic analysis for laminated composite beams. *Composite Structures*, vol. 44, pp. 81-87.

Bazant, Z. P. (2000): Structural stability. *International Journal of Solids and Structures*, vol. 37, pp. 55-67.

Bolotin, V. V. (1965): *The Dynamic Stability of Elastic Systems*, New York, Holden-Day Inc.

Chen, C. C.; Yeh, M. K. (1999): Parametric instability of a column with axially oscillating mass. *Journal of Sound and Vibration*, vol. 224, pp. 643-664

Chen, C. C.; Yeh, M. K. (2001): Parametric instability of a beam under electromagnetic excitation. *Journal of Sound and Vibration*, vol. 240, pp. 747-764

Chen, L. W.; Yang, J. Y. (1990): Dynamic stability of laminated composite plates by the finite element method. *Computers & Structures*, vol. 36, pp. 845-851.

Craig Jr., R. R. (1981): *Structural Dynamics*, New York, Wiley.

Deolasi, P. J.; Datta, P. K. (1995): Parametric instability characteristics of rectangular plates subjected to localized edge loading (compression or tension). *Computers & Structures*, vol. 54, pp. 73-82.

Deolasi, P. J.; Datta, P. K. (1997): Simple and combination resonances of rectangular plates subjected to non-uniform edge loading with damping. *Engineering Structures*, vol. 19, pp. 1011-1017.

Evan-Iwanowski, R. M. (1965): On the parametric response of structures. *Applied Mechanics Review*, vol. 18, pp. 699-702.

Fox, C. H. J. (1990): Parametrically excited instability in a lightly damped multi-degree-of-freedom system with gyroscopic coupling. *Journal of Sound and Vibration*, vol. 136, pp. 275-287

Ganapathi, M.; Balamurugan, V. (1998): Dynamic instability analysis of a laminated composite circular cylindrical Shell. *Computers & Structures*, vol. 69, pp. 181-189.

Gibson, R. F. (2007): *Principles of Composite Material Mechanics*, Boca Raton, FL, CRC Press

Hsu, C. S. (1963): On the parametric excitation of a dynamic system having multiple degrees of freedom. *Transactions of the ASME: Journal of Applied Mechanics*, vol. 30, pp. 367-372.

Moorthy, J.; Reddy, J. N. (1990): Parametric instability of laminated composite plates with transverse shear deformation. *International Journal of Solids and Structures*, vol. 26, pp. 801-811.

Nayfeh, A. H.; Mook, D. T. (1977): Parametric excitations of linear systems having many degrees of freedom. *Journal of Acoustical Society of America*, vol. 62, pp. 375-381.

Nayfeh, A. H. ; Mook, D. T.(1979): *Nonlinear Oscillations*, New York Wiley Inc.

Srinivasan, R. S.; Chellapandi, P. (1986): Dynamic stability of rectangular laminated composite plates. *Computers & Structures*, vol. 24, pp. 233-238.

Yeh, M. K.; Chen, C. C. (1998): Dynamic instability of a general column under periodic load in the direction of tangency coefficient at any axial position. *Journal of Sound and Vibration*, vol. 217, pp. 665-689.

Yeh, M. K.; Kuo, Y. T. (2004): Dynamic instability of composite beams under parametric excitation. *Composites Science and Technology*, vol. 64, pp. 1885-1893.

Yeh, M. K.; Tan, C. M. (1994): Buckling of elliptically delaminated composite plates. *Journal of Composite Materials*, vol. 28, no. 1, pp. 36-52.